Tr. J. of Physics
23 (1999) , 1051 – 1064.

Projectile Fragmentation in Emulsion at (4.1-4.5) A GeV/c

A.El-NAGHY, S. A. H. ABOU-STEIT
Physics Department, Faculty of Science,
Cairo University, Giza, EGYPT
M. MOHERY
Physics Department, Faculty of Science,
South Valley University, Sohag, EGYPT

Received 27.01.1999

Abstract

The fragmentation process has been investigated for 4.5A GeV/c ^{28}Si nuclei in emulsion and compared with the results of 4.5A GeV/c ^{24}Mg and 4.1A GeV/c ^{22}Ne in order to test the validity of the different theoretical models. It has been found that a single parameter distribution is insufficient to explain exactly the fragmentation process. Correlation studies have shown to be necessary for distinguishing between the different theoretical models for the fragmentation. The impact parameter, which defines the nature of the collision, has been found to influence considerably the shape of the charge yield distribution. The angular distributions of the projectile fragments can be described by quantum mechanical calculation.

Introduction

The fragmentation of colliding nuclei has shown to be an important process in studying high energy nuclear reactions e.g.[1-4]. The nuclear emulsion is a 4π-detector in which the projectile fragments are easily identified and their charges can be measured. The exact fragmentation mechanism is still a matter of debate. Three main mechanisms for the fragmentation of a heavy nucleus may be schematically distinguished [5]: first, the spallation in which the mass of the main fragment is close to that of the prefragment nucleus; second, the fission which yields two heavy fragments, each one having a mass almost equal to half the prefragment nucleus mass; and third, the multifragmentation in which many fragments are produced. Each one of these mechanisms is associated with a characteristic mass yield distribution and a certain temperature of the prefragment system [5-7]. The nuclear models for multifragmentation are mainly divided into two

main approaches: the first one implies the excitation of the prefragment nucleus and its evaporation [8-10]. The second is a statistical one, without any consideration of thermal equilibrium like the shattering of a stone into different pieces [11-13].

In the present work, all the projectile and the target fragments have been recorded and the data of the ^{28}Si collision with emulsion at 4.5A GeV/c have been analyzed for all fragments. A particular interest in the analysis, has been devoted to the study of the multiplicities and the correlations of the projectile fragments. Moreover, the angular and momentum distributions have been investigated.

Experimental Techniques

Nuclear emulsions of the type Br-2 were exposed to 4.5A GeV/c ^{28}Si beams at the Dubna Synchrophasotron. The pellicles of emulsion have the dimensions 20 cm $\times$ 10 cm $\times$ 600 μm (undeveloped). The intensity of the beam was about 10^4 particles/cm^2 and the beam diameter was approximately 1 cm. Along the track, a double scanning has been carried out fast in the forward direction and slow in the backward one.

The scanned beam tracks have been further examined by measuring the delta-electron density [14] on each of them to exclude any track having a charge less than the beam particle charge. Scanning has been performed using a Leitz-Laborlux-S microscope. According to the range L in the emulsion and the relative ionization $I^\star = I/I_0$, where I is the particle track ionization and l_0 is the ionization of a relativistic shower track in the narrow forward cone of an opening angle $\theta \leq 3^\circ$, the fragments are classified into the following groups [15]:

- Shower tracks producing "s-particles" having a relative ionization $I^\star \leq$1.4. Such tracks having an emission angle $\theta \leq 3^\circ$ have been further subjected to multiple scattering measurements for momentum determination [16] in order to separate the produced pions from the singly charged projectile fragments.
- Grey tracks producing "g-particles" having a relative ionization $I^\star \geq 1.4$ and $L > 3mm$.
- Black tracks producing "b-particles" having $L < 3mm$.

The classification of these particles, according to their kinetic energies (K.E.), is given in Table 1. The "b" and "g" tracks are both called heavily ionizing tracks producing "h-particles".

Table 1. Classification of particles according to their kinetic energies in MeV

Particle	Shower Particles	Grey Particles	Black Particles
π	$\geq$ 60	12<K.E.<60	$\leq$12
k	$\geq$ 212	20<K.E.<212	$\leq$20
^{1}H	$\geq$ 400	26<K.E.<400	$\leq$26
^{2}H	$\geq$ 800	36<K.E.<800	$\leq$36

The determination of the momentum of the s- particles emitted within $\theta \leq 3^\circ$ enables the separation of the produced pions from the non-interacting singly-charged projectile fragments (protons, deuterons and tritons) [17]. The g-particles emitted within $\theta \leq 3^\circ$ and having $L > 2cm$ are considered to be projectile fragments having Z=2. The b-particles

of $\theta \leq 3^\circ$ and $L > 1cm$ are due to projectile fragments having $Z \geq 3$. The number of delta-electrons has been measured for each of these particles in order to determine the corresponding charge $Z = 3, \ldots Z_b$.

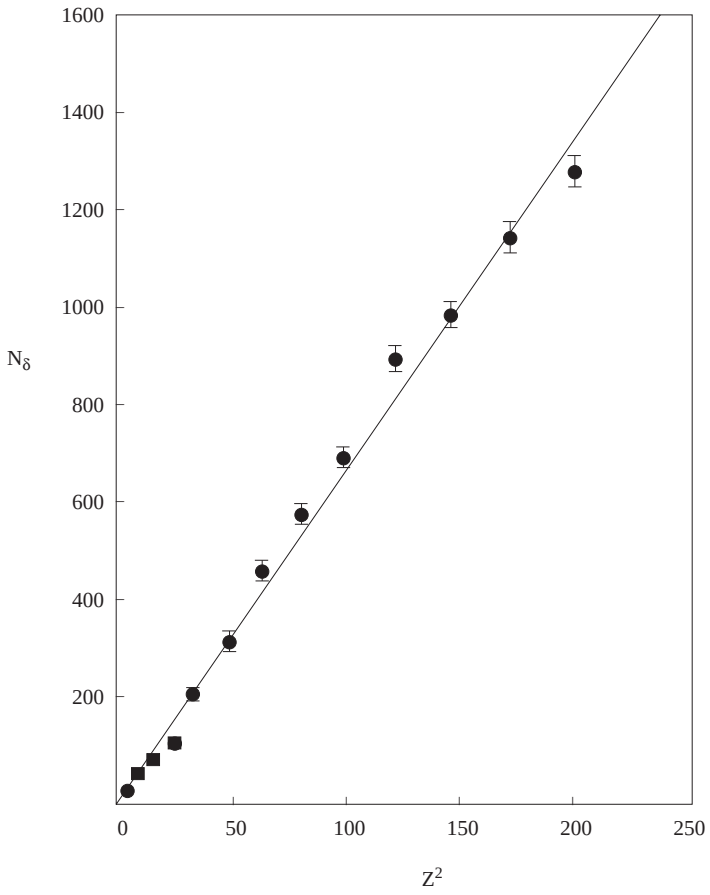

Figure 1. Dependence of N_δ the number of the delta-electrons of the projectile fragments on Z^2

Figure 1 shows the dependence of the number of the delta-electrons of the projectile fragments on the square of their charges. The value corresponding to a Z=2 projectile fragment has been used to check the validity of the relation between N_δ and Z^2.

Thus, all the particles have been adequately divided into: projectile fragment with Z varying from 1 to Z_b and target fragments, i.e., h-particles and the generated shower particles. The polar angle θ of each track, i.e., the space angle between the direction of the beam and that of the given track has been measured.

Multiplicities of Projectile Fragments and Correlations

A number of 2352 inelastic interactions of 4.5A GeV/c ^{28}Si nuclei with emulsion were picked up along a total scanned length of 240.2 m. The mean free path of the inelastic interactions has been found to be 9.9±0.3 cm. The inelastic cross-section has been compared to the calculations of the geometrical models and has shown to be consistent with the models [18,19]. A number of 2220 events have shown to be accompanied by projectile fragments, i.e. 94.4% of the total sample. The multiplicity distributions for Z=1, Z=2 and $Z \geq 3$ projectile fragments are shown in Fig. 2(a,b and c, respectively) compared to the corresponding distributions for 4.5A GeV/c ^{24}Mg collisions with emulsion [20]. The distributions for the two collisions are found to be consistent within experimental errors.

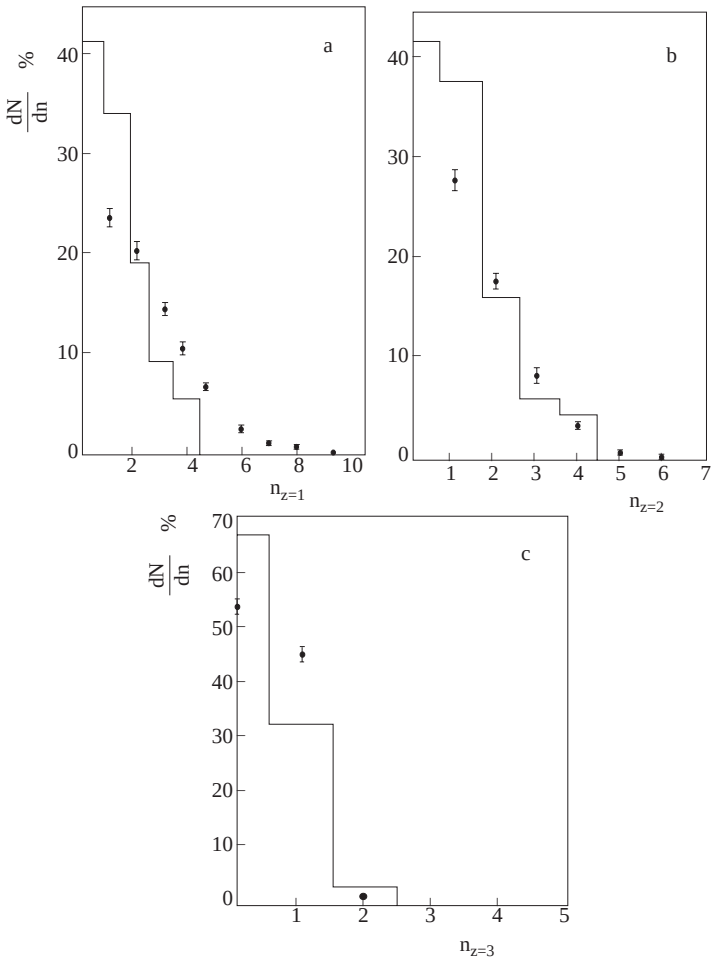

Figure 2. Multiplicity distributions of the projectile fragments for a) Z=1, b) Z=2 and c) Z≥3 for ^{28}Si (dots) and ^{24}Mg (solid histogram) at 4.5 A GeV/c

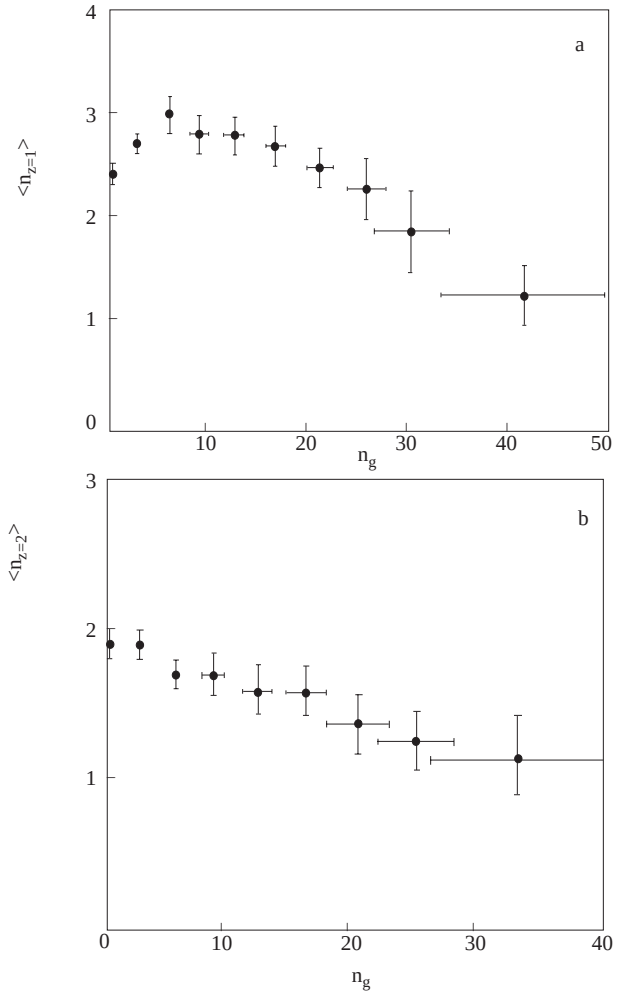

Figure 3. Average multiplicities of the projectile fragments as a function of n_g for a) Z=1 and b) Z=2 for ^{28}Si at 4.5 A GeV/c

The average multiplicities for the singly and doubly charged projectile fragments versus n_g are shown in Fig.3 (a and b). From the figure, it may be seen that the average multiplicity first increases slightly and then decreases for the singly charged more than for the doubly charged projectile fragments. The increase may be attributed to the extreme peripheral collisions where the projectile fragmentation is characterized by its nuclear structure, while the decrease may be due to the strong correlation between the projectile and the target fragmentation. When n_g increases, i.e. the impact parameter of the collision decreases, this allows a violent interaction in which both the target excitation energy and the temperature increase.

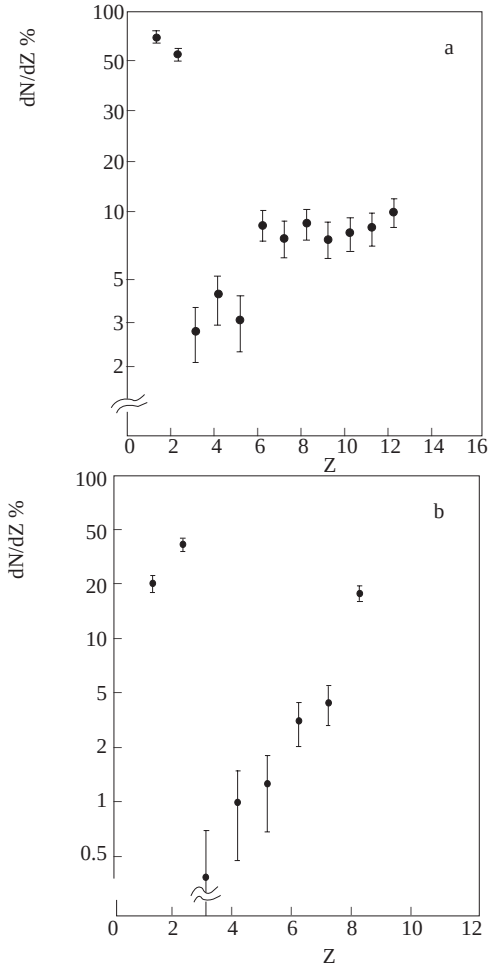

Figure 4. Charge yield distribution of the proijectile fragments having N_h=0 for a) 4.5 A GeV/c ^{28}Si and b) 4.1 A GeV/c ^{22}Ne

The dependence of the mechanism of the projectile fragmentation on the target fragmentation has been studied. Figure 4(a,b) shows the charge yield distributions for events having N_h=0 for 4.5 GeV/c ^{28}Si and 4.1 A GeV/c ^{22}Ne, respectively. In the very gentle collisions characterized by N_h=0, the energy transferred to the target nucleus is minimum. In most of these collisions, the projectile nucleus evaporates singly or doubly charged fragments and the residual nucleus is emitted as one big fragment. The charge yield distribution has a U-like shape resulting from the mixture of the characteristic shapes of the spallation and the fission mechanisms. In contrast, for $N_h \geq$6, Fig. 5 shows that the charge yield for 4.5 A GeV/c ^{28}si decreases with the increase of the charge of the

projectile fragment. This displays the correlation between the projectile and the target fragmentation. These $N_h \geq 6$ events are characterized by a high excitation energy of the target nucleus related to the violent projectile fragmentation process. The decrease of the charge yield distribution is considered as a typical feature of the multi-fragmentation mechanism. As a measure of the violence of the collision, the number of the singly charged projectile fragments n_1 and the value of the maximum charge Z_{max} of a projectile fragment in an event have been considered. Table 2 shows the charge yield distribution as a function of n_1. At the lower values of n_1 (0,1 and 2), the charge yield distribution first decreases then it increases according to a U-like shape while for n_1 ≥3 it is generally decreasing. The charge yield distribution decreases with the increase of the number of singly charged fragments. Table 3 illustrates how the charge yield distribution changes markedly with the variation of Z_{max}. The process of fragmentation of the projectile changes from being violent to become gentle with the increase of Z_{max}. From the tables, the intra-correlation between the projectile fragments appears to be evident.

Table 2. Charge distribution of the projectile fragments as a function of the number of the singly charged projectile fragments n_1

n_1 Z	0	1	2	3	4	5	6	7	8	9	10
1		555	478	343	245	120	65	31	15	2	2
2	187	324	277	229	164	83	42	19	8	1	2
3	13	25	21	25	16	8	1	3	1		
4	6	21	16	18	14	5	7	1		1	
5	7	23	33	19	13	4	1		1		
6	16	33	36	21	16	10	2	2			
7	25	41	31	20	8	6	1	1			
8	25	34	33	20	9	3		2			
9	29	60	31	16	8	3	1				
10	29	41	39	13	5						
11	33	36	22	5							
12	50	31	21	1				1			
13	38	25									
14	40	6	1								

Angular and Momentum Distributions

The angular distributions for Z=1,2 and ≥3 are shown in Fig.6(a,b and c, respectively). All the distributions are relatively narrow and the width of the distribution decreases with the increase of the charge of the projectile fragment. In high energy collisions, the fragmentation of nuclei has been treated by a quantum mechanical approach using the sudden approximation and the shell model functions [21]. It has been shown that the distribution of the momentum projections, in the projectile rest frame, are well

approximated to first order by a Gaussian-like distribution with a standard deviation width [22,23]

$$\Delta = [m\omega A_F(A_b - A_F)/2A_b]^{1/2} \quad MeV/c, \tag{1}$$

where A_b is the mass number of the beam nucleus, A_F is the fragment mass number, m is the proton mass in Mev and

$$\omega = 45A_b^{-1/3} - 25A_b^{-2/3}. \tag{2}$$

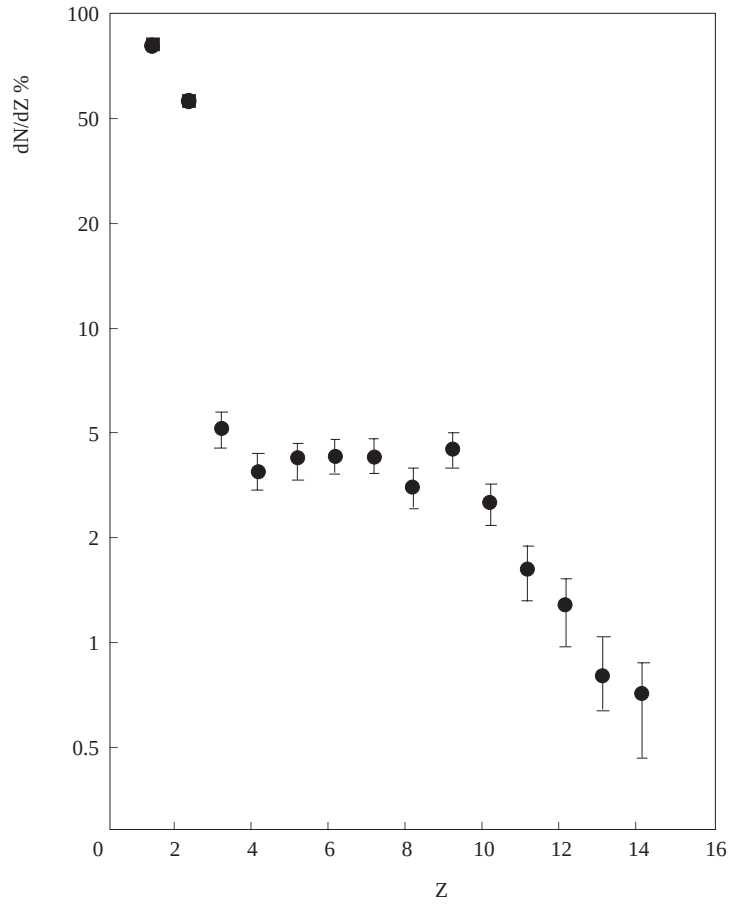

Figure 5. Charge yield distribution of the projectile fragments having $N_h \geq$=6 for ^{28}Si at 4.5 A GeV/c

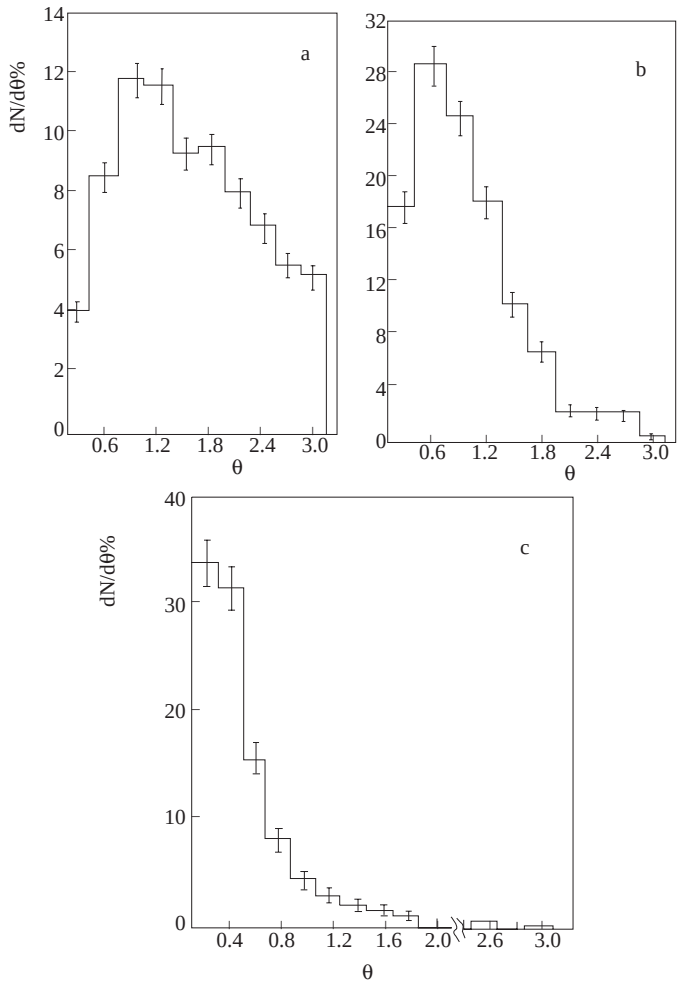

Figure 6. Multiplicity angular distributions of the projectile fragments for ^{28}Si at 4.5 A GeV/c for a) Z=1, b) Z=2 and c) Z≥3

The projection angle θ_{proj}, defined as the angle between the projection of the emitted particle track in the emulsion plane and the beam direction, has been determined in order to compare the experimental data with the theoretical calculations since the momenta of $Z > 1$ projectile fragments and the masses of all fragments have not been measured in this experiment. Figure 7(a,b) shows the $dN/d\theta_{proj.}$ distributions for the singly and doubly charged projectile fragments, respectively.

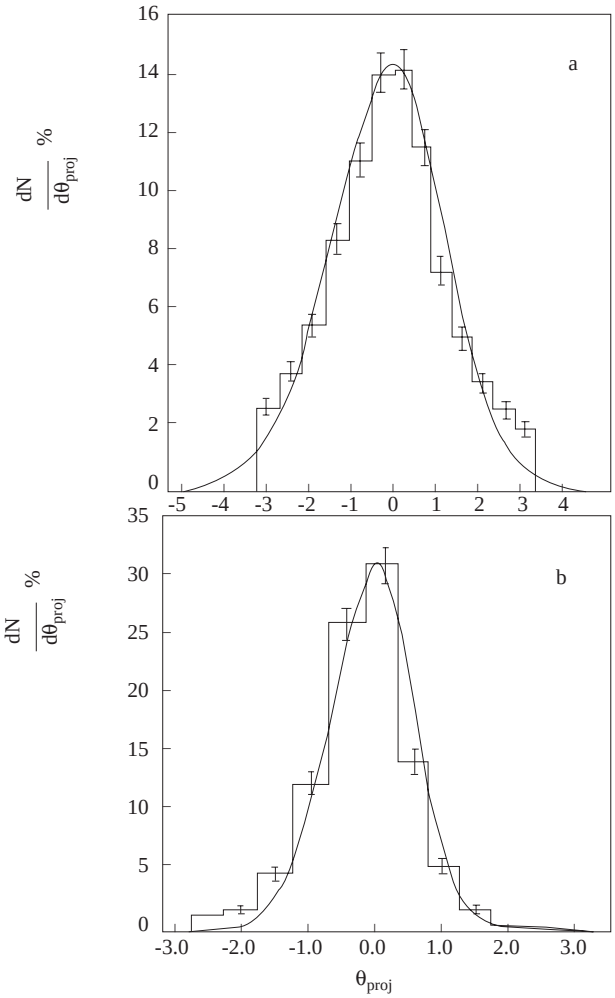

Figure 7. Projected angular distributions for a) Z=1 and b) Z=2 projectile fragment isotopes of ^{28}Si at 4.5 A GeV/c. The curve is the fitting of the experimental points by the Gaussian distribution (2)

The experimental points have been fitted to a Gaussian distribution of the form:

$$N(\theta_{proj.}) = Ce^{(-\theta^2_{proj.}/2\Delta^2_{proj})}, \tag{3}$$

where C is a constant and $\Delta_{\theta_{proj}}$ is a fitting parameter. The curves in Fig.7(a,b) represent the results of the fitting.

The values of Δ have been calculated according to equation (1), for fragments of different mass numbers A_F and are given in Table 4. The standard deviation width

of the corresponding projected angular distribution for these fragments $\delta_{\theta_{proj.}}$ has been calculated according to:

$$\delta_{\theta_{proj}}(deg) = 57.3\Delta/4500A_F. \quad (4)$$

A weight factor W has been given to each fragment isotope of charge Z corresponding to its fractional yield. The weight factors, obtained from the momentum measurements [17], have been used to calculate the standard deviation width of the angular distribution, $\Delta_{\theta_{proj.}}$ for the singly and doubly charged fragments. The results of the calculations are given in Table 4 in comparison with the corresponding values obtained from the fitting of the experimental data. This shows a good agreement between the experimental data and the calculations. This result agrees qualitatively with the previously obtained results in the ^{22}Ne collisions with emulsion at 4.1 A GeV/c [22]. The agreement of the experimental data with the theoretical calculations, for both interactions 4.5 A GeV/c ^{28}Si and 4.1 A GeV/c ^{22}Ne with emulsion, indirectly indicates the existence of a flow of the projectile fragments, i.e. their bounce-off.

Table 3. Dependence of charge distribution of projectile fragments on Z_{max}

Z_{max} Z	2	3	4	5	6	7	8	9	10	11	12	13	14
1	635	89	79	99	114	111	100	112	95	61	50	25	5
2	692	75	51	77	102	97	85	68	50	21	11	1	
3		94	2	6	5	3	1	1	1	1			
4			83	5	2		1						
5				97	1	2							
6					125		2						
7						131							
8							118				1		
9								138					
10									121				
11										94			
12											99		
13												62	
14													38

For further investigation of the sideward flow, a vector P_i=4.5 $A_i \sin\theta_i$ in the azimuthal plane has been attributed to each i^{th} projectile fragment and then these vectors have been summed up to obtain the resultant momentum vector of the projectile fragments. The resultant momentum vector of the target fragments has been obtained assuming a unit vector for each target fragment along its direction in the azimuthal plane. The resultant momentum vectors of the projectile and the target fragments have been determined for each event and each time the angle ϕ between them has been calculated. Figure 8 shows the distribution of the angle ϕ between the resultant momentum vectors

of the projectile and the target fragments. It can be seen that the distribution has a peak at approximately 180°, which means that the projectile and the target fragments are emitted in opposite directions. This result has been used as a signature of the flow of the nuclear matter [22,25] which is consistent with the hydrodynamical models for the nucleus-nucleus collisions [e.g.10-16,18,19,21,26-29].

Table 4. Standard deviation widths of the momentum (MeV/c) and angular distributions (degrees) of singly (Z=1) and doubly (Z=2) charged fragments

Z	Isotope	W	Δ	$\delta_{\theta_{proj.}}$	Calculated $\Delta_{\theta_{proj.}}$	Experimental $\Delta_{\theta_{proj.}}$
1	^{1}H	0.63	74.0	0.94		
1	^{2}H	0.27	102.7	0.65		
1	^{3}H	0.10	123.3	0.52		
					0.82	1.30±0.30
2	^{3}He	0.24	123.3	0.52		
2	^{4}He	0.76	139.5	0.44		
					0.46	0.60±0.02

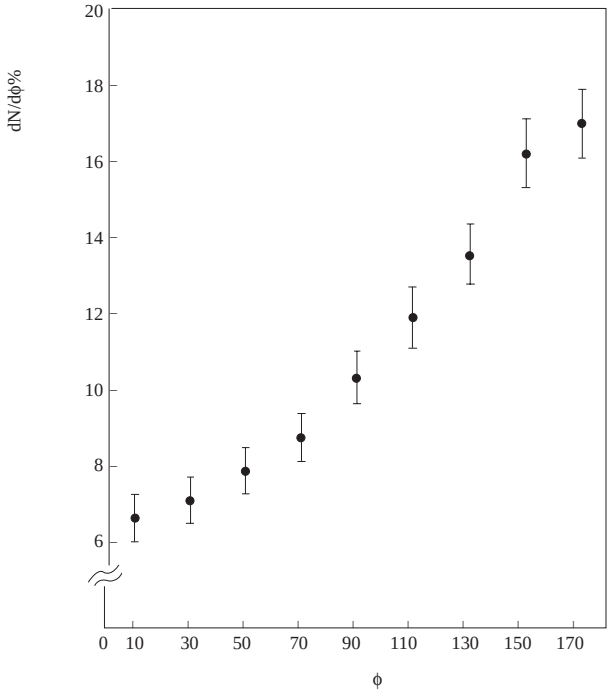

Figure 8. Distribution of the angle ϕ between the resultant vectors of the projectile and target fragments in azimuthal plane for ^{28}Si at 4.5 A GeV/c

Conclusions

The single parameter multiplicity or angular distribution is insufficient to reveal the mechanism of the fragmentation process. A strong correlation between the projectile and the target fragmentation processes has been observed in the multiplicity distributions. At small impact parameters, the fragmentation is violent while, in peripheral collisions, it is a gentle or soft process. Thus, the charge yield distribution may be described by the superposition of soft and violent collisions.

The angular distributions of the projectile fragments are typically narrow and their widths are strongly dependent on the fragment charge. The momentum distributions of the projectile fragments, in the rest frame of the prefragment system, have shown to be consistent with theoretical calculations. This consistency may assume the bounce-off of the projectile fragments.

References

[1] A. Schuttauf et al., Nucl Phys. **A607** (1996) 457.

[2] G. Giacomelli et al., Presented at the international Symposium on large Scale Collective Motions in Atomic Nuclei Brolo, Italy, 15-17 Oct.(1996)

[3] M. L. Cherry, et al., Z. Phys. **c73** (1997) 449.

[4] A. I. Bondarenko et al., Communications of JINR, P1-97-099.

[5] J. Hüfner, Phys. Rep. **125** (1985) 129.

[6] V. D. Toneev et al., Fiz. E. Ch. Atom. Yad. **17** (1986) 1093.

[7] I. N. Mishustin, Nucl. Phys. **A447** (1986) 67C.

[8] R. W. Minich et al., Phys. Lett. **118B** (1982) 458.

[9] D. H. E. Gross et al., Z. Phys. **A309** (1982) 42.

[10] W. A. Friedman and W. G. Lynch Phys. Rev. **C28** (1983) 950.

[11] J. Aichelin, Phys. Rev. **C30** (1984) 107.

[12] X. Campi et al., Phys. Lett. **142B** (1984) 8.

[13] J. Aichelin and J. Hufner, Phys. Lett. **136B** (1984) 15.

[14] C. F. Powell, P. H. Fowler and D. H. Perkins, Study of Elementary Particles by the Photographic Method (Pergamon Press, 1959) p.587.

[15] A. El-Naghy et al., Nuovo Cim. **107A** (1994)279.

[16] W. H. Barkas, Nuclear Research Emulsion I (New York Academic Press, 1963) p.388.

[17] Alma-Ata-Bucharest-Gatchina-Dubna-Dushanbe-Kosice-Cracow-Leningrad-Moscow-Tashkent-Tbilisi-Ulan-Bator-Yerevan Collaboration: Izvestiya AN SSSR, Ser. Fiz.**11** (1986) 2103.

[18] H. C. Bradt and B. Peters, Phys. Rev. **77** (1950) 54.

[19] P. J. Karol, Phys. Rev. **C11** (1975) 1203.

[20] N. N. Abd-Allah, Nucl.Sci.J.**30** (1993) 167.

[21] J. V. Lepore and R. J. Riddell, Report **LBL-3086** (1974).

[22] B. P. Bannik et al., Z. Phys. **A329** (1988) 341.

[23] H. H. Heckmann et al., Phys Rev. **C17** (1978)1735.

[24] A. El-Naghy et al., J. Phys. G. **14** (1988) 1125.

[25] J. Aichelin and X. Campi, Phys. Rev. **C34** (1986) 1643.

[26] R. Stock et al., Phys.Rev.Lett. **44** (1980) 1243.

[27] L. P. Csernai and W. Greiner, Phys.Lett.**99B** (1981) 85.

[28] H. A. Gustafsson et al., Phys.Rev.Lett.**52** (1984) 1590.

[29] R. E. Rendfordt et al., Phys.Rev.Lett.**53** (1984) 763.